Available online at www.sciencedirect.com
ScienceDirect
Trans. Nonferrous Met. Soc. China 23(2013) 3040−3045
Transactions of Nonferrous Metals Society of China
www.tnmsc.cn

Cycle life prediction and match detection in retired electric vehicle batteries

Xiang-yang ZHOU[1], You-lan ZOU[1], Guang-jin ZHAO[2], Juan YANG[1]

1. School of Metallurgy and Environment, Central South University, Changsha 410083, China;
2. Electric Power Research Institute, Henan Electric Power Corporation, Zhengzhou 450052, China

Received 14 September 2012; accepted 21 January 2013

Abstract: The lifespan models of commercial 18650-type lithium ion batteries (nominal capacity of 1150 mA·h) were presented. The lifespan was extrapolated based on this model. The results indicate that the relationship of capacity retention and cycle number can be expressed by Gaussian function. The selecting function and optimal precision were verified through actual match detection and a range of alternating current impedance testing. The cycle life model with high precision (>99%) is beneficial to shortening the prediction time and cutting the prediction cost.

Key words: retired electric vehicle battery; life prediction model; match detection; electrochemical impedance spectroscopy; equivalent circuit

1 Introduction

The leaping development of electric vehicles in the near future will promote large-scale production of lithium ion batteries (LIBs) [1,2]. LIBs retired from electric vehicles are widely reused for their residual capacities as high as 80% of the designed capacities. A reasonable way to predict the residual life of the retired batteries is beneficial to classifying the batteries, realizing cascade utilization and reducing environment pollution [3].

Presently, the physical performance of LIBs has been thoroughly studied, but there are scarcely any reports about the prediction of their residual life. Most researchers have started with life modeling from analyzing the physical properties and validated its precision by entire life test [4−7]. THOMAS et al [8] presented a degradation model that focused on the degradation rate rather than the accumulated degradation. ZHANG and WHITE [9] used a physics-based single particle model to simulate the cycle life of the LIBs. They have divided the capacity loss into three stages: the formation of solid-state electrolyte film, the loss of active cathode material and the intercalation of the cathode. Therefore, the limiting factors have been determined before simulation based on this theoretical principle [10,11]. However, the battery often suffers time-varying capacity in real-time running, leading to the inconsistency of the different batteries [12]. For example, the environment temperature and charging/discharging regulations occasionally alter [13,14]. After the monomer battery is retired, it is a more complicated process to obtain battery life. In order to make the best use of the residual capacity, it is necessary to design an optimal degradation track for the battery. This is also a meaningful study on the longevity and the cycle life prediction of the batteries.

Electrochemical impedance spectroscopy (EIS) is one of the most effective methods to investigate LIBs without destruction of the battery. It is always used to study the electrodes in a relatively wide frequency domain. The fast speed of sub-processes appears in the high frequency area, while the slower speed appears in the low frequency area. Thus, the dynamic characteristics would be discussed separately according to each sub-process. The equivalent circuit and its parameters are introduced to express the structure of LIB's resistance. In order to verify the validity of the model, the variation tendency of the resistance in different states was investigated [15−17].

In this work, the entire life model for the batteries

Foundation item: Projects (51204209, 51274240) supported by the National Natural Science Foundation of China: Project (HNDLKJ[2012]001-1) supported by Henan Electric Power Science &Technology Supporting Program, China
Corresponding author: Juan YANG; Tel: +86-731-88836329; E-mail: zylan0935@csu.edu.cn
DOI: 10.1016/S1003-6326(13)62831-9

was obtained and verified by the charging/discharging test, rate-capability test and cycle life test. Backward induction was applied in pursuit of the reasons that generated the model function. Then, the electrochemical impedance spectroscopy was introduced to build the relations between the capacity fading and resistance so as to verify the validation of the model.

2 Experimental

2.1 Charging/discharging test

The fabricated 1.15 A·h class 18650-type cylindrical cells were used to measure the charge/discharge curves during cycling. The active materials of the cells were $LiFePO_4$ for the positive electrode coated on aluminum foil and hard carbon for negative electrode coated on copper foil. 1 mol/L $LiPF_6$ in solvent of ethylene carbonate (EC)/ diethyl carbonate (DMC)/ethyl methyl carbonate (EMC) (1:1:1, in volume) was used as electrolyte. The electrochemical experiments were performed between the lower cut-off potential of 2.0 V and the upper cut-off potential of 3.85 V using a LAND testing (CT2001C, Wuhan Jinluo Electron Co., Ltd., China). All of the six batteries were charged at rate of 1*C* and every two batteries were tested under the same discharge rate (5*C*, 10*C* or 15*C*). The scheme of the life cycle test of LIBs was shown as the following four patterns:

1) After keeping static state for 10 min, the battery was charged at 1*C* until the voltage is up to 3.85 V, then it was charged at this potential until the current dropped to 0.057 mA;

2) The battery reached static state after 10 min and underwent discharging test at 5*C*, 10*C* or 15*C* to 2.0 V, respectively;

3) The procedures above were repeated until the discharge number（that is cycle number）at 5*C* is up to 600 cycles, 10*C* to 80% of the designed capacity, 15*C* to 80% of the designed capacity;

4) The data were recorded and analyzed by computer. The two batteries tested at 5*C* were marked as 1-5*C*-1 and 1-5*C*-2. For comparison, the two batteries tested at 10*C* and 15*C* were marked as 1-10*C*-1, 1-10*C*-2, 1-15*C*-1 and 1-15*C*-2, respectively.

2.2 Electrochemical impedance spectroscopy test

A new retired battery was charged at 1*C* and discharged at 5*C* until the discharge number is up to 600 cycles. The electrochemical impedance spectroscopy (EIS) test was proceeded when the battery was tested every 40 or 50 cycles The frequency range of the EIS test was from 100 kHz to 10 mHz and the electrochemical multi-channel test system (Solartron 1470E, Sdartron Mettology Co., Ltd., USA) was chosen for this test.

3 Results and discussion

3.1 Cycle life degradation simulation

Figure 1 presents the curves of the original capacity fading and the corresponding simulation models at different discharge rates of 5*C*, 10*C* and 15*C*. As time proceeds, the rate of capacity loss changes. The capacity loss during cycle test exhibits the irreversible component. That is, the capacity loss cannot be recovered through charging the battery. For this reason, the shape of the capacity retention versus cycle number is similar to that of the discharge capacity versus cycle number. It can be seen that the original discharge curves of the six batteries keep a similar pattern. The three-stage pattern about capacity retention is clearly seen in Fig. 1(a). The discharge capacity rises in the initial stage for the positive and negative electrodes are not completely activated. The discharge capacity decreases with the cycle number increasing, indicating that the irreversible expansion occurs at the positive electrode and the severe oxidation occurs at the negative electrode. The speed of the capacity fading is initially low in the second stage,

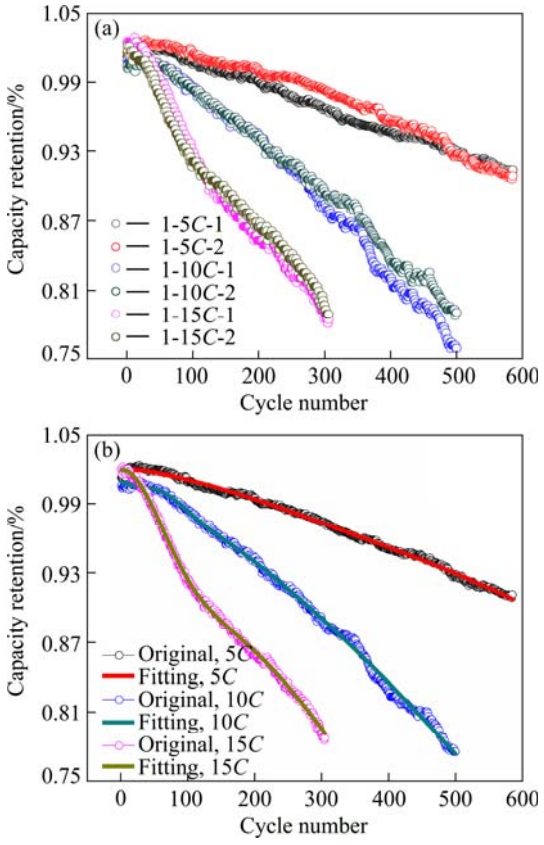

Fig. 1 Original capacity fading curves (a) and corresponding simulation models (b) at different discharge rates of 5*C*, 10*C* and 15*C*

but deteriorates quickly after a few hundreds of cycles in the third stage. It must be noted that the actual capacity output declines gradually and the speed of capacity attenuation becomes quick with the increase of discharge rate (from 5*C* to 15*C*). It is because some electro-chemical reactions cannot occur at higher discharge rates, leading to the decrease of discharge capacity. However, there is no significant difference in discharge capacity for the two cells tested under the same discharge rates. Therefore, it is necessary to take the average operation to build the relationship between the capacity retention and the cycle number. The relationship is shown in Fig. 1(a). The average discharge capacity and simulated discharge capacity as a function of cycle number are shown in Fig. 1(b). The battery model acceptably replicates the performance of the real battery with a reasonable degree of accuracy at high discharge rates (15*C*). However, the battery model becomes less accurate at lower rates of discharge (5*C*, 10*C*), possibly because of the side reactions which occur at low rates and change the discharge capacity.

The capacities of the LIBs above emerge some degree of attenuation over a period of store or use. So it is necessary to design an optimal degradation track before use. The reliability assessment of the lithium-ion battery is realized based on the prediction track without actual testing data. Figure 2 shows the curves of the entire life prediction of the batteries. The degradation tracks can be fitted by the second Gaussian function. Equation (1) with different parameters (Table 1) is used to show the numerical relationships between the capacity retention and the cycle number, and characterize the capacity degradation model of LIBs under different discharge conditions.

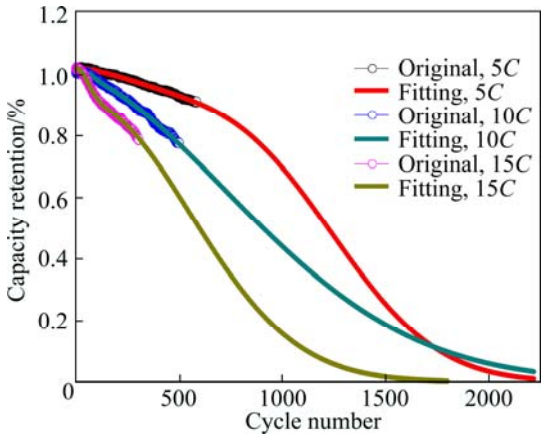

Fig. 2 Cycle life prediction of capacity fading at different discharge rates of 5*C*, 10*C* and 15*C*

$$C_N=a_1\exp\left[-\left(\frac{N-b_1}{c_1}\right)^2\right]+a_2\exp\left[-\left(\frac{N-b_2}{c_2}\right)^2\right] \quad (1)$$

where C_N represents the discharge capacity in the N cycles; a_1, b_1, c_1, a_2, b_2, c_2 are the simulated constants of the model, respectively. When the end of life is defined to be 80% of the designed capacity, the maximum cycle number of the cells at different rates of 5*C*, 10*C* and 15*C* are estimated to be 850, 458 and 295 cycles, respectively. In order to reuse the batteries, it is significant to predict battery's residual life at the shortest cost (as few charge-discharge cycle times as possible). According to the prediction curves, the prediction reliability and accuracy of the models depend on the quantity of the tested data.

3.2 Cycle life degradation match detection

The working situation of a given battery before retired has a strong influence on the residual life. The fitting tracks of the capacity fading can be used to develop a model-base to predict lifespan under different operation conditions. It is necessary to select the optimal model from the model-base with a small amount of data, and control the simulation precision in a permissible limit. Considering the given curves in Fig. 3 as the standard models, another retired battery was selected and the vector $\boldsymbol{d}=(d_1, d_2, \cdots, d_m)$, ($m$=15−40) was used to represent the match data, where d_m represents the discharge capacity in the m cycles. The concrete match method is as follows:

1) The vector $\boldsymbol{d}$ was introduced to each model, and the position of the vector $\boldsymbol{d}$ in each model was determined and should be closest to the model's fade trend;

2) The optimal position that should be closest to the model's fade trend was found out from the determined positions of each model above.

The follows are the calculation steps of the match algorithm.

1) The length of the vector was calculated.

2) The continuous values of m variables in each model were calculated. That is, $C_i=(p_{i1}, p_{i2}, \cdots, p_{im})$, $p_{ij}=C_{i+j-1}$, i=1, 2, $\cdots$, k_1, j=1, 2, $\cdots$, m. C_i represents a

Table 1 Simulation parameters of cycle life prediction

Rate	a_1	b_1	c_1	a_2	b_2	c_2	R^2
5*C*	0.9462	−183.4	810.4	0.6137	853.6	671.7	0.9966
10*C*	9.001×10^{-3}	65.62	42.05	1.034	−203.1	1305	0.9977
15*C*	0.1135	−0.4065	81.25	0.9078	33.21	733	0.9988

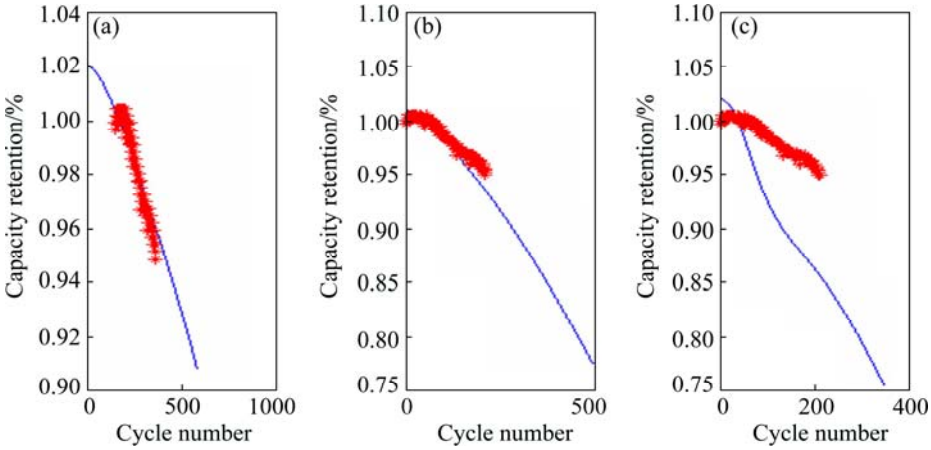

Fig. 3 Actual match results in 5*C* (a), 10*C* (b) and 15*C* (c) models

series of random and continuous capacity values of m variables; p_{ij} represents one of the capacity value and its relative position is the same as d_j. i and k_1 represent the calculating number and the maximum calculate number of each model, respectively.

3) The minimum value was found out between all of the C_i and the vector in a special norm (such as the second norm) under each model; Y=min($||C_1-d||_2$, $||C_2-d||_2$, ⋯, $||C_{k1}-d||_2$); Y represents the minimum value based on the spectral norm.

4) The minimum value was found out from the obtained minimum among the three models.

The model with the final minimum value is the desired model to match, and its corresponding i is the starting time of the cycle numbers. Therefore, the residual life of the battery can be presented as model life $-i$.

In order to verify the accuracy of the algorithm, a series of data were selected as shown in Fig. 3. Taking 10*C* for instance, the starting data obtained from actual measurement is 65, and the actual residual life is 307 to failure threshold. However, according to the above algorithm, the results are a little different. The starting data in the 10*C* model is 62, and the residual life is 310 to failure threshold. The mach detention is about 99.03%.

3.3 Electrochemical impedance spectroscopy analysis

The external failure type of the battery is demonstrated by the capacity loss in the forms of the second Gaussian function. In order to test the inter failure type that is caused by the cells' resistance, a cell is tested by electrochemical impedance spectroscopy (EIS). The typical EIS spectrum of the chosen cell is tested at the full state of charge and the equivalent circuit is used to fit the spectra in Fig. 4.

Different electrochemical reactions usually occur at specific frequency intervals. From Fig. 4, the EIS spectrum can be divided into three stages: 1) The porous

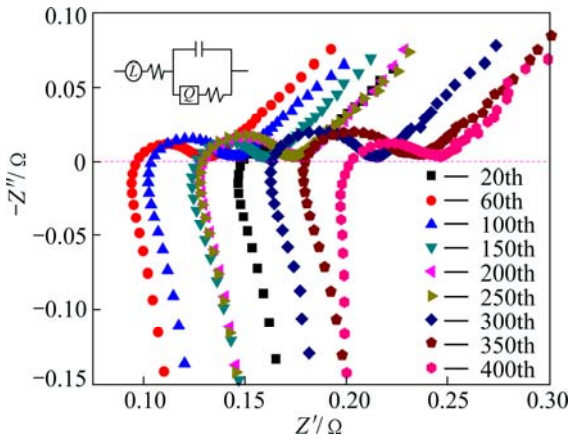

Fig. 4 Typical EIS spectra of tested cell after every 40 or 50 cycles

and non-uniformity characters on the surface of the electrodes that generate the inductive resistance at a very low frequency; 2) Lithium ion transport and charge transfer at the electrode/electrolyte interface that lead to a semicircle at mi-frequency; 3) The formation of electrolyte impedance and interface film at high frequency.

The equivalent circuit is presented to complete the fitting processes. It is comprised of an inductor L and an intercept R_1 at a high frequency, a capacitor C paralleled with a resister R_2 and so-called constant phase element CPE at a mid-low frequency.

It is found from Table 2 that the best fitting results with the lowest error (up to 10%) can be obtained for the battery charging/discharging after 20 cycles. The fitting values are effectively shown the changes as expected.

According to Fig. 5, the resistances of R_1 and R_2 decrease at early cycles, then increase gradually with the increase of the cycles and abruptly deteriorate when the battery life is retired. The value of R_1 decreases with cycling for the stable electrode/electrolyte interface film (SEI film) is formed in the first stage, and the

Table 2 Fitting error of cell after 20 cycles

Item	L/H	R_L/Ω	C/(μF·cm^{-2})	Q/(Ω^{-1}·cm^{-2}·s^n)	f/Hz	R_1/Ω
Before fitting	2.3×10^{-7}	0.1004	33	57.89	0.5505	2.4×10^{-2}
After fitting	2.3×10^{-7}	0.1004	3.3×10^{-3}	58.85	0.5505	2.4×10^{-2}
Error/%	1.763	0.8367	9.74	3.537	3.301	4.266

Table 3 Simulation parameters of resistance change

Resistance	a_3	b_3	c_3	a_4	b_4	c_4	R^2
R_1	0.1678	658.5	498.1	2.275×10^{13}	−1578	276.3	0.9655
R_2	0.04451	437	315.6	6.219×10^{11}	−1334	243.9	0.9835
R_1+R_2	0.197	545.2	408.7	2.381×10^{13}	−1380	243.2	0.9747

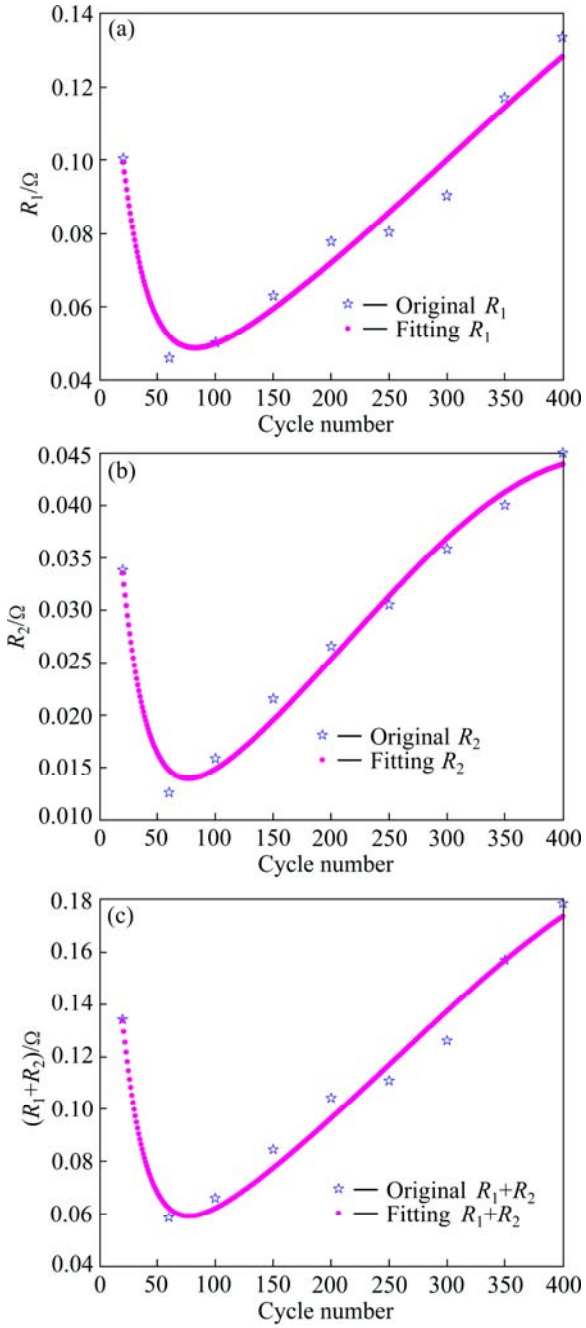

Fig. 5 Curves of original resistance R_1 (a), R_2 (b), R_1+R_2 (c) and fitting results based on cycle number

electrolyte is sufficient for lithium ion transportation. The value of the R_2 also reduces with cycling for the intact structure of the electrodes is beneficial to the lithium ion transportation at the electrolyte/electrode interface and inter-electrode. After the cell experiencing a certain degree of degradation, the value of R_1 rises because of the electrolyte consumption. The value of R_2 also increases. This is because the electrode of the cell undergoes sever polarization reaction, and the damaged SEI film during lithium ions insertion and extraction is continually repaired.

Equation (2) with different parameters (Table 3) was used to show the numerical relationships with cycle; a_3, b_3, c_3, a_4, b_4, c_4 are the simulated constants of characterize impedance spectroscopy model.

$$R=a_3\exp\left[-\left(\frac{N-b_3}{c_3}\right)^2\right]+a_4\exp\left[-\left(\frac{N-b_4}{c_4}\right)^2\right] \quad (2)$$

where R represents the resistance of the battery in the N cycles; a_3,b_3,a_4,b_4,c_4 are the simulated constants of the model, respectively.

From the function above, it can be seen that the accuracy of the model depends on the quantity of the test data. The resistance change meets the second Gaussian function. Comparing with Eq. (1), it is interesting to found that the cell has the same function expression between the capacity degradation and the resistance change (vs cycle number). This shows the battery performance depends on the capacity loss and the increase of resistance. Before 80 cycles, the capacity of the cell rises and the resistance deduces. After that, the capacity of the cell reduces and the resistance rises. Therefore, it is significant to build a model from both the internal and external factors of the cell in order to test the validity of the prediction models.

4 Conclusions

The cycle life of LIBs can be accurately estimated

based on establishment of the prediction model-base. The capacity decays nonlinearly as a function of discharge cycles. The functional form of the model follows Guassian path. Match detection verifies that the optimal precision is high to 99%. The failure form of the impedance that acquires from an equivalent circuit fitting also complies with the second Gaussian relations.

References

[1] GONDELACH S J G, FAAIJ A P C, Performance of batteries for electric vehicles on short and longer term [J]. Journal of Power Sources, 2012, 212(15): 111−129.

[2] HE Hong-wen, XIONG Rui, GUO Hong-qiang. Online estimation of model parameters and state-of-charge of $LiFePO_4$ batteries in electric vehicles [J]. Applied Energy, 2012, 89(1): 413−420.

[3] ZACKRISSON M, AVELLĂN L, ORLENIUS J. Life cycle assessment of lithium-ion batteries for plug-in hybrid electric vehicles-Critical issues [J]. Journal of Cleaner Production, 2010, 18(15): 1519−1529.

[4] STAMPS A T, HOLLAN C E, WHITE R E, GATZKE E P. Analysis of capacity fade in a lithium ion battery [J]. Journal of Power Sources, 2005, 150(4): 229−239.

[5] SHRIHARI S, BALAJI K. A capacity fade model for lithium-ion batteries including diffusion and kinetics [J]. Electrochimica Acta, 2012, 70(1): 248−254.

[6] SCHMIDT A P, BITZER M, IMRE Ă W, GUZZELLA L. Model-based distinction and quantification of capacity loss and rate capability fade in Li-ion batteries [J]. Journal of Power Sources, 2010, 195(22): 7634−7638.

[7] TAKEI K, KUMAI K, KOBAYASHI Y, MIYASHIRO H. Cycle life estimation of lithium secondary battery by extrapolation method and accelerated aging test [J]. Journal of Power Sources, 2001, 97(1): 697−701.

[8] THOMAS E V, BLOOM I, CHRISTOPHERSEN J P, BATTAGLIA V S. Rate-based degradation modeling of lithium-ion cells [J]. Journal of Power Sources, 2012(206): 378−382.

[9] ZHANG Q, WHITE R E. Capacity fade analysis of a lithium ion cell [J]. Journal of Power Sources, 2008(179): 793−798.

[10] WANG Zhi-fu, ZHANG Cheng-ning. Auto-test on motor temperature rising in electric vehicles with mutual MRAS [J]. Journal of Beijing Institute of Technology, 2008, 17(4): 395−399. (in Chinese)

[11] ANDREW T S, CHARLES E H, PALPH E W, EDWARD P G. Analysis of capacity fade in a lithium ion battery [J]. Journal of Power Sources, 150(4): 229−239.

[12] ERNESTO M R, RUBEN V M, ANTONIO F T. Modeling and simulation of lithium-ion batteries [J]. Computers and Chemical Engineering, 2011, 35(1): 1937−1948.

[13] KUO R J, WANG C F, CHEN Z Y. Integration of growing self-organizing map and continuous genetic algorithm for grading lithium-ion battery cells [J]. Applied Soft Computing, 2012, 12(1): 2012−2022.

[14] HU Chao, BYENG D Y, CHUNG J. A multiscale framework with extended Kalman filter for lithium-ion battery SOC and capacity estimation [J]. Applied Energy, 2012, 92(1): 694−704.

[15] WU Mao-sung, LIN Chang-yen, WANG Yung-yun, WAN Chi-chao. Numerical simulation for the discharge behaviors of batteries in series and/or parallel-connected battery pack [J]. Electrochimica Acta 2006, 52(1): 1349−1357.

[16] GAO Fei, LI Jian-lin, ZHAO Shu-hong, WANG Zi-dong. Research progress on lithium-ion power battery life prediction [J]. Electronic Components & Materials, 2009, 28(6): 79−83.

[17] OSAKA T, MOMMA T, MUKOYAMA D, HARA H. Proposal of novel equivalent circuit for electrochemical impedance analysis of commercially available lithium ion battery [J]. Journal of Power Sources, 2012, 205(1): 483−486.

退役动力电池寿命预测与匹配检验

周向阳[1]，邹幽兰[1]，赵光金[2]，杨 娟[1]

1. 中南大学 冶金与环境学院，长沙 410083；

2. 河南电网 电力研究院，郑州 450052

摘 要：研究商业用 18650 型锂离子电池(额定容量 1150 mA·h)的循环寿命衰减规律，利用外推法预测电池的剩余寿命。结果表明，锂离子电池容量保持率与循环寿命服从二次高斯函数关系，匹配检测和一系列的交流阻抗测试验证了所选择的模型的正确性以及精度(>99%)。建立循环寿命模型有利于缩短电池寿命测试周期，降低预测成本。

关键词：退役动力电池；寿命预测模型；匹配检验；电化学阻抗谱；等效电路

(Edited by Xiang-qun LI)